

論文 / 著書情報
Article / Book Information

Title	Low-temperature field-effect and magnetotransport properties in a ZnO based heterostructure with atomic-layer-deposited gate dielectric
Authors	A. Tsukazaki,A. Ohtomo,D. Chiba,Y. Ohno,H. Ohno,M. Kawasaki
Citation	Applied Physics Letters, Vol. 93, No. 24,
Pub. date	2008, 12
URL	http://scitation.aip.org/content/aip/journal/apl
Copyright	Copyright (c) 2008 American Institute of Physics

Low-temperature field-effect and magnetotransport properties in a ZnO based heterostructure with atomic-layer-deposited gate dielectric

A. Tsukazaki,^{1,a)} A. Ohtomo,¹ D. Chiba,^{2,3} Y. Ohno,³ H. Ohno,^{2,3} and M. Kawasaki^{1,4,5}

¹*Institute for Materials Research, Tohoku University, Sendai 980-8577, Japan*

²*Semiconductor Spintronics Project, Exploratory Research for Advanced Technology (ERATO), Japan Science and Technology Agency, Tokyo 102-0075, Japan*

³*Laboratory for Nanoelectronics and Spintronics, Research Institute of Electrical Communication, Tohoku University, Sendai 980-8577, Japan*

⁴*WPI Advanced Institute for Materials Research, Tohoku University, Sendai 980-8577, Japan*

⁵*Japan Science and Technology Agency (CREST), Tokyo 102-0075, Japan*

(Received 24 September 2008; accepted 5 November 2008; published online 17 December 2008)

A top-gate field-effect device with atomic-layer-deposited Al_2O_3 dielectric was fabricated to investigate magnetotransport properties of two-dimensional electron gas (2DEG) at a semi-insulating $\text{ZnO-Mg}_{0.12}\text{Zn}_{0.88}\text{O}$ double heterostructure grown by laser molecular-beam epitaxy. Hall mobility monotonically increased as the density of accumulated electrons increased. The highest mobility at 2 K was recorded to be $5000 \text{ cm}^2 \text{ V}^{-1} \text{ s}^{-1}$ at a 2DEG density of $1.2 \times 10^{12} \text{ cm}^{-2}$, which is comparable to the previously reported value for a metallic $\text{ZnO/Mg}_{0.2}\text{Zn}_{0.8}\text{O}$ heterostructure. Insulator-to-metal transition was observed at a critical density of $6 \times 10^{11} \text{ cm}^{-2}$. The metallic-state channel exhibited Shubnikov-de Haas oscillations, demonstrating an electric-field tunable quantum device based on transparent oxide semiconductor. © 2008 American Institute of Physics. [DOI: 10.1063/1.3035844]

Transparent conducting oxides (TCOs) have technological potential for realizing transparent electronics. In the past decade, thin film transistors consisting of ZnO and related compounds have been intensively studied for improving device characteristics.¹⁻³ To date, key parameters of amorphous or polycrystalline channel devices, such as on-off ratio and field-effect mobility, approach a practical level for flat-panel display applications. The development of additional applications will be enabled by the improved performance of single-crystalline channel devices.⁴⁻⁷ In spite of many intriguing aspects at the fundamental research level, however, there are very few attempts of investigating low-temperature magnetotransport in field-effect transistors (FETs). In practice, it is also an essential approach for the improvement of device performance as well as understanding device physics.^{8,9} The recent observation of the quantum Hall effect in $\text{Mg}_x\text{Zn}_{1-x}\text{O/ZnO}$ heterostructures opens a promising opportunity for such a study.^{10,11} One of the particular interests is field-effect control of Landau filling factor in two-dimensional electron gas (2DEG).

In this system, the 2DEG is spontaneously accumulated at the interface by the mismatch in electric polarization between the $\text{Mg}_x\text{Zn}_{1-x}\text{O}$ barrier and the ZnO well.¹⁰⁻¹⁴ The 2DEG density can be controlled with varying Mg content and donor concentration in the well layer. The growth polarity (O or Zn polar) is a primary factor because it determines the directions of the spontaneous and piezoelectric polarizations and resulting potential energy gradient. Two configurations are possible to induce 2DEG at the interfaces: the O-polar ZnO on $\text{Mg}_x\text{Zn}_{1-x}\text{O}$ and the Zn-polar $\text{Mg}_x\text{Zn}_{1-x}\text{O}$ on ZnO. There are several reports for both cases, where the former is grown by laser molecular-beam epitaxy (L-MBE),¹⁰ whereas the latter is grown by MBE.^{11,15,16}

In this study, we employed atomic-layer-deposited amorphous Al_2O_3 gate dielectric to accumulate 2DEG in an O-polar double heterostructure, where polarization mismatch was designed to be very small.¹⁰ Atomic layer deposition (ALD) attracts increasing interest, owing to its superiority for preparation of reliable gate dielectrics on a wide spectrum of materials.¹⁷⁻²¹ High breakdown field and low trap density make it possible to perform stable measurements under high electric field. By the use of ALD Al_2O_3 , we have successfully attained the 2DEG density of $1.2 \times 10^{12} \text{ cm}^{-2}$. The accumulated 2DEG exhibited clear insulator-to-metal transition²² (IMT) and Shubnikov-de Haas (SdH) oscillations below quantum resistance $h/e^2 \sim 25.8 \text{ k}\Omega$, where h is Planck's constant and e is the elementary charge.

The $\text{ZnO-Mg}_x\text{Zn}_{1-x}\text{O}$ double heterostructure was prepared on insulating (0001) ScAlMgO_4 substrate. A high-purity ZnO single crystal (ZN technology, Brea CA) and a homemade $\text{Mg}_{0.06}\text{Zn}_{0.94}\text{O}$ ceramic target were ablated by a KrF excimer laser (5 Hz, 1 J/cm^2) at 1×10^{-6} Torr of oxygen. The sample consists of a top layer of 50-nm-thick $\text{Mg}_{0.12}\text{Zn}_{0.88}\text{O}$, a 100-nm-thick ZnO layer, and a bottom layer of 100-nm-thick $\text{Mg}_{0.12}\text{Zn}_{0.88}\text{O}$. The bottom $\text{Mg}_{0.12}\text{Zn}_{0.88}\text{O}$ layer was grown at 650°C and annealed at 1000°C in 1 mTorr of oxygen to make its surface atomically flat.²³ The growth temperature (T_g) for the ZnO layer and the top $\text{Mg}_{0.12}\text{Zn}_{0.88}\text{O}$ layer was set at 950°C . Standard Hall bars with a channel area of $60 \times 260 \mu\text{m}^2$ were fabricated by using Ar ion etching and conventional photolithography technique. Using an ALD apparatus, a 40-nm-thick amorphous Al_2O_3 gate dielectric was deposited at 150°C .²⁰ Ohmic and gate electrodes consisting of Au/Ti layers were electron beam evaporated. Low-temperature magnetotransport measurements were carried out with lock-in technique in a physical property measurement system (Quantum Design). A series standard resistance of $1 \text{ M}\Omega$ was inserted into the measurement circuit for current correction.

^{a)}Electronic mail: tsukaz@imr.tohoku.ac.jp.

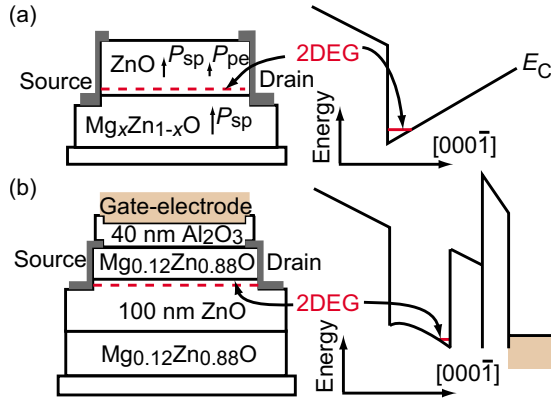


FIG. 1. (Color online) Schematic of cross-sectional device structures (left) and conduction band diagrams (right) for (a) previously reported ZnO/Mg_{0.2}Zn_{0.8}O heterostructures and (b) field-effect device used in this study. For the former, the 2DEG, spontaneously formed at bottom of the top ZnO layer, leads to metallic conduction. For the latter, the 2DEG is accumulated at the top interface under positive gate bias.

Figure 1 illustrates the difference in sample structures, conduction band diagrams, and locations of 2DEG between previously examined metallic heterostructures (top) and the present field-effect device (bottom) studied here. Both samples have the same configurations (O polar, compressively strained ZnO layers, and unstrained Mg_xZn_{1-x}O layers), and the directions of spontaneous (P_{sp}) and piezoelectric polarization (P_{pe}) are upward toward the surface. When x is higher than ~ 0.1 , the sum of $|P_{sp}|$ and $|P_{pe}|$ in ZnO layer is considerably smaller than $|P_{sp}|$ in Mg_xZn_{1-x}O. Therefore, positive charges formed at the bottom ZnO/Mg_xZn_{1-x}O interface induce 2DEG in the side of ZnO.¹⁰ As shown in Fig. 1(a), this is the case for the metallic heterostructures with $x \geq 0.15$, given with sufficiently high donor concentrations in ZnO grown at high T_g (for example, 1000 °C at $x = 0.15$).^{10,24} In this study, we chose a set of parameters of both relatively lower x and T_g , which is expected to result in nearly flatband and low donor concentration in the ZnO layer. In fact, the bottom channel was “off” for the present film, exhibiting a semi-insulating conduction without gating, and a metallic “on” state appeared under applied positive gate bias, as will be described below. This clearly indicates that 2DEG was accumulated at the top of ZnO layer with electric field gating through atomic-layer-deposited Al₂O₃, a high mobility channel being formed at the clean epitaxial interface with top Mg_xZn_{1-x}O layer [see Fig. 1(b)].

Our device showed a typical n -type FET behavior in its output characteristics. Figure 2(a) shows drain current (I_D) versus drain voltage (V_D) measured at 2 K after each incremental change of gate voltage (V_g) by 1 V. Systematic V_g dependence of longitudinal resistance (ρ_{xx}) shown in the inset indicates that carriers were accumulated at the top interface. Through all of the measurements, gate leakage current was suppressed below 10 pA.

Hall effect was measured at 2 K by applying magnetic field up to ± 1 T, V_g ranging from 2 to 8 V, and an ac excitation of 1 μ A. Note that the Hall effect in the linear region was sufficiently characterized under the given ranges of V_g and I_D . Both of carrier density (n) and mobility (μ) increased with increasing V_g but the increase in the latter was more dramatic due to the rapid evolution of screening effect [Fig. 2(b)]. n could be increased up to 1.2×10^{12} cm⁻² by applying $V_g = 8$ V. From linear V_g dependence of n , we extracted an

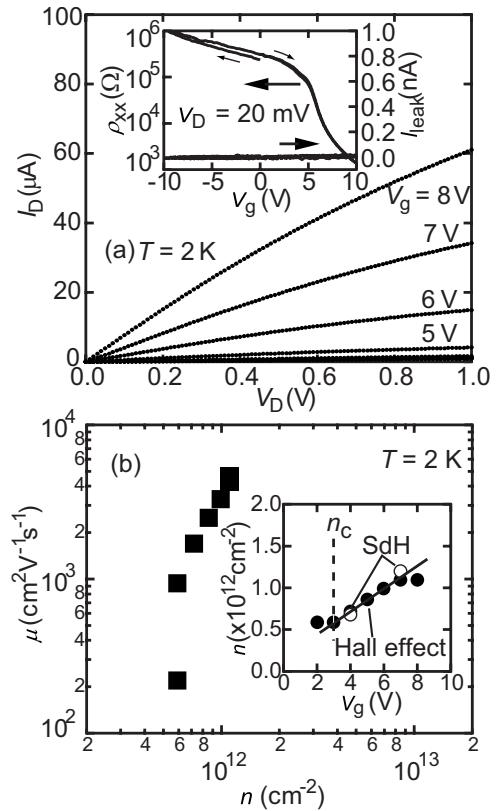


FIG. 2. Field- and Hall-effect characteristics of the FET device at 2 K. (a) Output curves measured in a V_g range of -2 to 8 V. The inset shows V_g dependence of ρ_{xx} and leakage current. (b) Electron mobility (μ) as a function of 2DEG density (n) evaluated from Hall effect (closed circles). The 2DEG density evaluated from SdH oscillations is also plotted by open circles. Inset depicts V_g dependence of n . Straight line is a linear fit. Critical carrier density (n_c) of the IMT is $\sim 6 \times 10^{11}$ cm⁻² (broken line).

effective capacitance of stacking layers (40-nm-thick Al₂O₃ and 50-nm-thick Mg_{0.12}Zn_{0.88}O) to be ~ 20 nF/cm². Indeed, the highest value of μ was recorded to be 5000 cm² V⁻¹ s⁻¹ at $V_g = 7$ V, which is comparable to those for a metallic ZnO/Mg_{0.2}Zn_{0.8}O heterostructure grown by using the same L-MBE system.¹⁰ Thus, it is concluded that the location of 2DEG does not affect the magnitude of μ in our devices.

We note that all of our L-MBE-grown films exhibit lower μ than that obtained for Zn-polar films grown by MBE (14000 cm² V⁻¹ s⁻¹).¹¹ It is most likely due to the difference in concentrations of unintentionally doped impurities such as Si and Al in Mg_xZn_{1-x}O barrier layers. In fact, the Mg_xZn_{1-x}O ceramic targets as starting materials for L-MBE growth have inevitable large amounts of the impurities, which also reflects its optical properties inferior to that of the MBE-grown Mg_xZn_{1-x}O.^{23,25–27} Therefore, the MBE-grown sample is much suitable to further study the field-effect control of 2DEG, which will be published elsewhere.

Figure 3 shows temperature dependence of ρ_{xx} measured at zero magnetic field by applying V_g ranging from -2 to 6 V. Insulating behavior ($d\rho_{xx}/dT < 0$) was seen when $V_g \leq 2$ V, while the metallic on state ($d\rho_{xx}/dT > 0$) appeared when $V_g \geq 4$ V. We note that the IMT took place below quantum resistance h/e^2 , which is consistent with the behavior expected for a two-dimensional system around 2 K.²² From Fig. 2(b), a critical carrier density (n_c) is identified to be $\sim 6 \times 10^{11}$ cm⁻², which is comparable to that observed for a photoinduced IMT in a ZnO/Mg_{0.15}Zn_{0.85}O heterostructure.²⁸ Compared to conventional 2DEG systems,

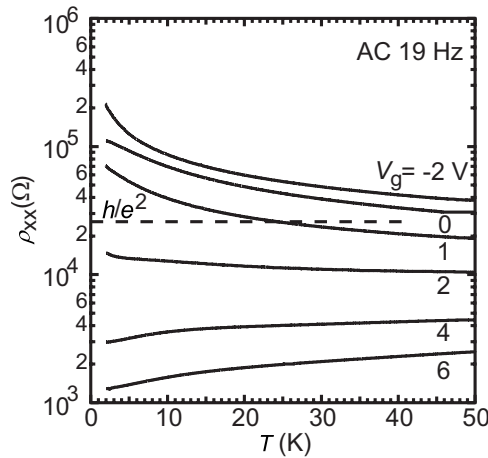


FIG. 3. Temperature dependence of longitudinal resistivity ρ_{xx} measured in a V_g range of -2 – 6 V by using a standard lock-in technique under ac excitation (12–20 nA, 19 Hz).

the observed n_c is one order of magnitude higher but it will be decreased if μ is improved.

Figure 4(a) shows typical magnetoresistance curves exhibiting SdH oscillations. The 2DEG density calculated from oscillation periods f as $n_{\text{SDH}} = 2fe/h$ shows good agreement with n evaluated from Hall effect [see Fig. 2(b)], indicating that the accumulated electron is well confined at the interface. The Hall resistance (ρ_{xy}) did not exhibit flat plateaus due to a high measurement temperature but it is consistent that weak shoulders corresponded to the ρ_{xx} minima.

In conclusion, we have studied magnetotransport of two-dimensional electrons in $\text{ZnO-Mg}_{0.12}\text{Zn}_{0.88}\text{O}$ double heterostructure by the use of atomic-layer-deposited gate dielectric. Unlike room-temperature characteristics in previously reported TCO based FETs, low-temperature mobility of our device showed remarkably large enhancement, more than one order of magnitude as carrier density was doubled from $6 \times 10^{11} \text{ cm}^{-2}$. As a result, μ reached $5000 \text{ cm}^2 \text{ V}^{-1} \text{ s}^{-1}$ across clear IMT, which confirms current upper bound for μ attainable in L-MBE-grown FETs. Ionized or neutral impurities in $\text{Mg}_x\text{Zn}_{1-x}\text{O}$ layers are thought to be predominant carrier scattering centers. Although the observed SdH oscillations and Hall plateaus were not very clear, partly due to

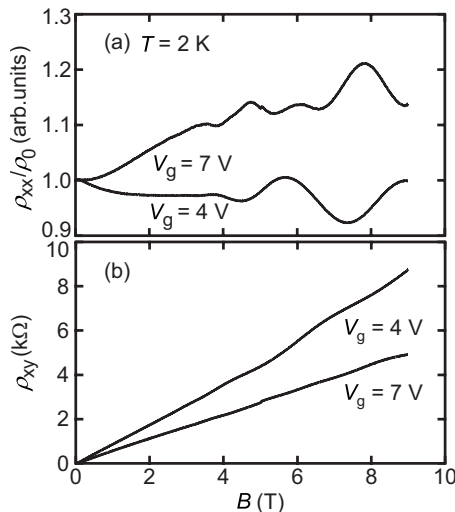


FIG. 4. (a) Magnetoresistance normalized by the values at zero magnetic field (ρ_{xx}/ρ_0) and (b) Hall resistance (ρ_{xy}) measured at 2 K for $V_g = 4$ and 7 V.

high temperature measurement, our experiments clearly demonstrate the possibility of electric-field control of quantum phase transition in diluted 2DEG at oxide semiconductor heterointerface.

The work was supported in part by the Murata Science Foundation and the Asahi Glass Foundation.

- ¹J. Nishii, F. M. Hossain, S. Takagi, T. Aita, K. Saikusa, Y. Ohmaki, I. Ohkubo, S. Kishimoto, A. Ohtomo, T. Fukumura, F. Matsukura, Y. Ohno, H. Koinuma, H. Ohno, and M. Kawasaki, *Jpn. J. Appl. Phys., Part 2* **42**, L347 (2003).
- ²K. Nomura, H. Ohta, A. Takagi, T. Kamiya, M. Hirano, and H. Hosono, *Nature (London)* **432**, 488 (2004).
- ³H. Kumomi, K. Nomura, T. Kamiya, and H. Hosono, *Thin Solid Films* **516**, 1516 (2008).
- ⁴K. Nomura, H. Ohta, K. Ueda, T. Kamiya, M. Hirano, and H. Hosono, *Science* **300**, 1269 (2003).
- ⁵T. I. Suzuki, A. Ohtomo, A. Tsukazaki, F. Sato, J. Nishii, H. Ohno, and M. Kawasaki, *Adv. Mater. (Weinheim, Ger.)* **16**, 1887 (2004).
- ⁶J. Nishii, A. Ohtomo, K. Ohtani, H. Ohno, and M. Kawasaki, *Jpn. J. Appl. Phys., Part 2* **44**, L1193 (2005).
- ⁷K. Koike, I. Nakashima, K. Hashimoto, S. Sasa, M. Inoue, and M. Yano, *Appl. Phys. Lett.* **87**, 112106 (2005).
- ⁸K. Shibuya, T. Ohnishi, T. Uozumi, T. Sato, M. Lippmaa, M. Kawasaki, K. Nakajima, T. Chikyow, and H. Koinuma, *Appl. Phys. Lett.* **88**, 212116 (2006).
- ⁹H. Nakamura, H. Takagi, I. H. Inoue, Y. Takahashi, T. Hasegawa, and Y. Tokura, *Appl. Phys. Lett.* **89**, 133504 (2006).
- ¹⁰A. Tsukazaki, A. Ohtomo, T. Kita, Y. Ohno, H. Ohno, and M. Kawasaki, *Science* **315**, 1388 (2007).
- ¹¹A. Tsukazaki, H. Yuji, S. Akasaka, K. Tamura, K. Nakahara, T. Tanabe, H. Takasu, A. Ohtomo, and M. Kawasaki, *Appl. Phys. Express* **1**, 055004 (2008).
- ¹²O. Ambacher, J. Smart, J. R. Shealy, N. G. Weimann, K. Chu, M. Murphy, W. J. Schaff, L. F. Eastman, R. Dimitrov, L. Wittmer, M. Stutzmann, W. Rieger, and J. Hilsenbeck, *J. Appl. Phys.* **85**, 3222 (1999).
- ¹³Supporting online material in Ref. 10.
- ¹⁴A. Malashevich and D. Vanderbilt, *Phys. Rev. B* **75**, 045106 (2007).
- ¹⁵K. Koike, K. Hama, I. Nakashima, G. Takada, M. Ozaki, K. Ogata, S. Sasa, M. Inoue, and M. Yano, *Jpn. J. Appl. Phys., Part 2* **43**, L1372 (2004).
- ¹⁶H. Tampo, H. Shibata, K. Matsubara, A. Yamada, P. Fons, S. Niki, M. Yamagata, and H. Kanie, *Appl. Phys. Lett.* **89**, 132113 (2006).
- ¹⁷P. D. Ye, G. D. Wilk, J. Kwo, B. Yang, H. J. Gossmann, M. Frei, S. N. G. Chu, J. P. Mannaerts, M. Sergeant, M. Hong, K. K. Ng, and J. Bude, *IEEE Electron Device Lett.* **24**, 209 (2003).
- ¹⁸K. Lai, P. D. Ye, W. Pan, D. C. Tsui, S. A. Lyon, M. Muhlberger, and F. Schaffler, *Appl. Phys. Lett.* **87**, 142103 (2005).
- ¹⁹T. M. Lu, J. Liu, J. Kim, K. Lai, D. C. Tsui, and Y. H. Xie, *Appl. Phys. Lett.* **90**, 182114 (2007).
- ²⁰D. Chiba, F. Matsukura, and H. Ohno, *Appl. Phys. Lett.* **89**, 162505 (2006).
- ²¹P. F. Carcia, R. S. McLean, and M. H. Reilly, *Appl. Phys. Lett.* **88**, 123509 (2006).
- ²²E. Abrahams, S. V. Kravchenko, and M. P. Sarachik, *Rev. Mod. Phys.* **73**, 251 (2001).
- ²³A. Tsukazaki, A. Ohtomo, S. Yoshida, M. Kawasaki, C. H. Chia, T. Makino, Y. Segawa, T. Koida, S. F. Chichibu, and H. Koinuma, *Appl. Phys. Lett.* **83**, 2784 (2003).
- ²⁴A. Tsukazaki, A. Ohtomo, and M. Kawasaki, *Appl. Phys. Lett.* **88**, 152106 (2006).
- ²⁵H. Yuji, K. Nakahara, K. Tamura, S. Akasaka, A. Sasaki, T. Tanabe, H. Takasu, T. Onuma, S. F. Chichibu, A. Tsukazaki, A. Ohtomo, and M. Kawasaki, *Proc. SPIE* **6895**, 68950D (2008).
- ²⁶M. Kubota, T. Onuma, A. Tsukazaki, A. Ohtomo, M. Kawasaki, T. Sota, and S. F. Chichibu, *Appl. Phys. Lett.* **90**, 141903 (2007).
- ²⁷Y. Nishimoto, K. Nakahara, D. Takamizu, A. Sasaki, K. Tamura, S. Akasaka, H. Yuji, T. Fujii, T. Tanabe, H. Takasu, A. Tsukazaki, A. Ohtomo, T. Onuma, S. F. Chichibu, and M. Kawasaki, *Appl. Phys. Express* **1**, 091202 (2008).
- ²⁸A. Tsukazaki, A. Ohtomo, M. Nakano, and M. Kawasaki, *Appl. Phys. Lett.* **92**, 052105 (2008).